Preturbulent Regimes in Graphene Flow

M. Mendoza,[1,*] H. J. Herrmann,[1,†] and S. Succi[2,‡]

[1]ETH Zürich, Computational Physics for Engineering Materials, Institute for Building Materials, Schafmattstrasse 6, HIF, CH-8093 Zürich, Switzerland

[2]Istituto per le Applicazioni del Calcolo CNR, Via dei Taurini, 19 00185, Rome, Italy, and Freiburg Institute for Advanced Studies, Albertstrasse, 19, D-79104, Freiburg, Germany

(Received 21 December 2010; published 14 April 2011)

We provide numerical evidence that electronic preturbulent phenomena in graphene could be observed, under current experimental conditions, through current fluctuations, echoing the detachment of vortices past localized micron-sized impurities. Vortex generation, due to micron-sized constriction, is also explored with special focus on the effects of relativistic corrections to the normal Navier-Stokes equations. These corrections are found to cause a delay in the stability breakout of the fluid as well as a small shift in the vortex shedding frequency.

DOI: 10.1103/PhysRevLett.106.156601 PACS numbers: 72.80.Vp, 47.11.−j, 47.75.+f

Since its recent discovery [1], graphene has continued to surprise scientists with an amazing series of spectacular properties, such as ultrahigh electrical conductivity, ultralow viscosity to entropy ratio, combination of exceptional structural strength and mechanical flexibility, and optical transparency. Many of these fascinating effects are due to the fact that, consisting of literally a single carbon monolayer, graphene represents the first instance of a truly two-dimensional material (the "ultimate flatland" [2]). Moreover, due to the special symmetries of the honeycomb lattice, electrons in graphene are shown to behave like an effective Dirac fluid of *massless* chiral quasiparticles propagating at a Fermi speed of about $v_F \sim c/300 \sim 10^6$ m/s. This configures graphene as a very special, slow-relativistic electronic fluid, where many unexpected quantum-electrodynamic phenomena can take place [3]. In particular, the capability of reaching down viscosity to entropy ratios smaller than that of superfluid helium at the lambda point has recently spawned the suggestion that electronic transport in graphene may support preturbulent phenomena [4].

In this Letter, we pursue this suggestion in quantitative terms. More precisely, we simulate the relativistic graphene-fluid equations, proposed in Ref. [4], under conditions of present and prospective experimental realizability. Our main result is that microscale impurities, as small as a few microns, are capable of triggering coherent patterns of vorticity in close qualitative and quantitative resemblance with classical two-dimensional turbulence (see, e.g., Fig. 1). It is also shown that such vorticity patterns give rise to detectable current fluctuations across the sample, well in excess of flickering noise. Since these current fluctuations lie in the range of several hundred MHz, their actual detection may still raise an experimental challenge. As a result, based on our simulations, we conclude that the hydrodynamic picture of graphene as a near-perfect, slow-relativistic fluid, as developed in Ref. [4], should be liable to experimental verification.

The equations for the Dirac electron fluid in graphene read as follows [4]: $\partial\rho_c/\partial t + \nabla\cdot(\rho_c\vec{u}) = 0$, for charge conservation, $\partial\epsilon/\partial t + \nabla\cdot[(\epsilon + p)\vec{u}] = 0$, for energy density conservation, and

$$\frac{\epsilon + p}{c^2}\left[\frac{\partial\vec{u}}{\partial t} + (\vec{u}\cdot\nabla)\vec{u}\right] + \nabla p + \frac{\vec{u}}{c^2}\frac{\partial p}{\partial t} - \eta\nabla^2\vec{u} = 0, \tag{1}$$

for momentum conservation. Here, c is the Fermi speed ($\sim 10^6$ m/s), ϵ the energy density, p the pressure, ρ_c the charge density, and $\vec{u}$ the velocity. The shear viscosity can be calculated by using [4]

$$\eta = C_\eta \frac{N(k_B T)^2}{4\hbar c^2 \alpha^2}, \tag{2}$$

where $C_\eta \sim O(1)$ is a numerical coefficient, T is the temperature, $\alpha = e^2/\varepsilon\hbar c$ is the effective fine structure

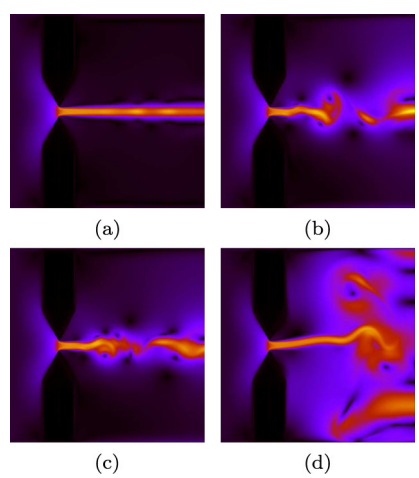

FIG. 1 (color online). Preturbulence at Re = 25 in graphene is shown at 379 400 time steps (a) and (b), and at 603 400 time steps (c) and (d). For (b) and (d) the term $\partial p/\partial t$ was removed. The color represents the magnitude of the velocity.

 © 2011 American Physical Society

constant, e being the electric charge of the electron, ε the relative dielectric constant, and N the number of species of free massless Dirac particles. Additionally, the entropy density can be calculated according to the Gibbs-Duhem relation $\epsilon + p = Ts$. These equations have been derived under the assumption $|\vec{u}| \ll c$. The relativistic lattice Boltzmann (RLB), proposed by Mendoza *et al.* [5], is hereby adapted to reproduce, in the continuum limit, the equations for the Dirac electron fluid described above. The RLB model [5] was defined on a three-dimensional lattice with 19 discrete velocities. Since graphene is two dimensional, we have adapted the model to a two-dimensional cell with nine discrete velocities, linking each site to its four nearest neighbors, four next-to-nearest neighbors (diagonal), plus a rest particle. The shear viscosity, according to this model, is $\eta = (\epsilon + p)(\tau - \frac{1}{2})c_l^2 \delta t/3c^2$, where $c_l = \delta x/\delta t$ is the ratio of the lattice spacing to time-step size and τ is the single relaxation time [5].

We choose the equation of state $\epsilon = 3p$, which depends on temperature in the relativistic regime, as $\epsilon \sim (k_B T)^3/(c\hbar)^2 = T^3$ (in normalized units $c = \hbar = k_B = e = 1$) [6]. Thus, the shear viscosity η would depend on the third power of the temperature, leading to a different relation than Eq. (2). However, in the Dirac fluid, the relaxation time for the electrons depends on the inverse of the temperature, $\tau_{\rm rel} = (\hbar\alpha)^2/k_B T$ [7], and, therefore, introducing this dependence into the relaxation time τ of the numerical model, we obtain the correct function for the viscosity. In numerical units ($\delta x = \delta t = c = 1$), we set the relaxation time to $\tau = \tau_0 T_0/T + 1/2$, where T_0 is the initial temperature and τ_0 the initial relaxation time.

The hydrodynamics equations are similar to the nonrelativistic Navier-Stokes equations with the exception of the compressibility term $\sim \partial p/\partial t$. This term is most likely negligible at low frequencies, but it may become relevant at higher ones. The Reynolds number Re, measuring the strength of inertial versus dissipative terms [4], is given by $\mathrm{Re} = (sT/c^2)(LU_{\rm typ}/\eta)$, where L and $U_{\rm typ}$ are the characteristic length and flow velocity of the system, respectively. In lattice units, it reads as

$$\mathrm{Re} = \frac{3LU_{\rm typ}}{c^2 \delta t(\tau - 1/2)}. \tag{3}$$

According to classical turbulence theory, vortex shedding in graphene is expected for Reynolds numbers well above 1, typically Re $\sim$ 10–100. To detect signatures of preturbulent behavior in graphene experiments, one can measure the fluctuations of the electric current through the graphene sample. The current density is defined by $\vec{j} = \rho_c \vec{u}$, and the total electric current is calculated integrating the current density along the transverse (y) coordinate. The characteristic fluctuation frequency can then be related to the vortex shedding frequency. Macroscopic speeds $u \sim 10^5$ m/s could be achieved by the electrons in graphene [8]. The Reynolds number rewrites as $\mathrm{Re} = U_{\rm typ} LT/c^2(\eta/s)$. According to Ref. [4], η/s takes values around $0.2\hbar/k_B$, at temperature of 300 K, so that we can write $\mathrm{Re} = U_{\rm typ} L/\nu_{\rm eff}$, $\nu_{\rm eff} = c^2\eta/Ts \sim 0.005$ m^2/s being the effective kinematic viscosity. Therefore, a sample of size $L = 5$ μm, within reach of current technology, would yield Re $\sim$ 100, sufficiently high to trigger preturbulent phenomena, such as vortex shedding. To test the idea on quantitative grounds, we implement a simulation on a grid with 1024×512 cells. The following initial values (numerical units) were used: $\epsilon = 0.75$, $\rho_c = 1.0$, $\vec{u} = (u_x, 0) = (0.002, 0)$, and the Fermi speed $c = c_l = 1.0$. The initial value of the relaxation time was chosen $\tau_0 = 0.003$ such that the initial shear viscosity $\eta = \frac{1}{3}(\tau - \frac{1}{2}) = 10^{-3}$.

A circular obstacle, with diameter $D = 50$, is introduced at (256, 256), modeling a 5 μm diameter impurity in the graphene sample (Fig. 2). With this configuration, and setting $L = D$ in Eq. (3), the Reynolds number for this system is Re $\sim$ 100. We choose periodic boundary conditions at top and bottom, and demand that the distribution functions of the boundary cells are always equal to the equilibrium distribution functions evaluated with the initial conditions. Free boundary conditions are imposed at the outlet. At the left border, we set inlet conditions, where the missing information of the distribution functions is filled by the equilibrium distribution function corresponding to the initial conditions [9]. We define $\delta t = 0.05$ ps.

The drag F_{Dx} and lift F_{Dy} forces acting on the obstacle are measured, the vortex shedding frequency being computed in terms of fluctuations of the lift forces. We compare the frequency of the electric current fluctuations with the frequency of the drag force, which, in general, is twice the vortex shedding frequency (see Fig. 3). To relate these to the vortex shedding, we use a fast-Fourier transform (FFT). As is well visible from Fig. 3, the current fluctuations contribute about one part per thousand of the base signal, and, consequently, they should be liable to experimental detection. In future applications, involving larger graphene samples, higher Reynolds numbers will be attained. Consequently, it becomes of interest to assess the role of the relativistic corrections to the classical Navier-Stokes equations.

Comparing the dynamics of the relativistic and n onrelativistic fluids, two basic differences emerge: the relativistic correction term $\sim \partial p/\partial t$ and the viscosity dependence with the temperature, Eq. (2). In order to assess

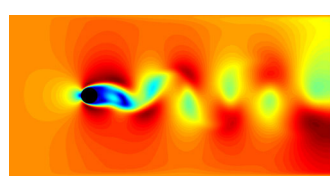

FIG. 2 (color online). Vortex shedding in graphene at Re = 100, using a grid of 1024×512 cells. The color scale represents the absolute velocity of the fluid.

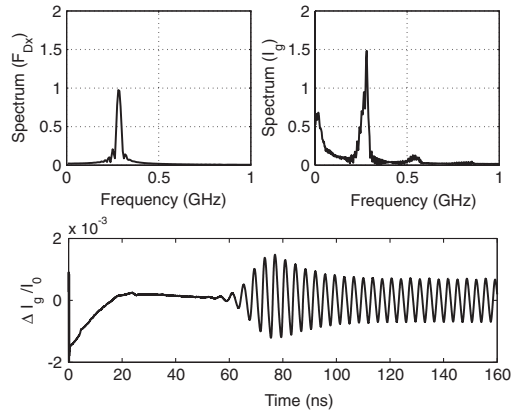

FIG. 3. FFT of the electric current fluctuations ΔI_g, in the graphene sample (top right), due to the vortex shedding as a function of time. Also, the FFT of the drag force acting on the obstacle is shown (top left). This result refers to Re = 100. At the bottom, the fluctuations in the electric current I_g are shown as a function of time.

whether these terms play an important role, we implement three simulations on a grid of size 2048×1024 cells. In the first simulation, we model the full relativistic equations; in the second one, the relativistic effect $\sim \partial p/\partial t$ is removed; and in the third one, the viscosity is forced to be a constant. The same initial configuration as before is used with the exception of $\vec{u} = (u_x, 0) = (0.03, 0)$ and $D = 100$ (in this case, modeling an impurity of diameter 150 μm). The impurity is now centered at (512, 512). With this configuration, Eq. (3) gives Re $\sim$ 3000. The simulations run up to 10^6 time steps (with $\delta t = 1.5$ ps).

From Fig. 4, we find that, in the case of constant viscosity, the frequency is a bit higher than the one corresponding to the full relativistic case. On other hand, if the term $\sim \partial p/\partial t$ is removed from the equations, the frequency decreases. We conclude that, in order to compare to high precision measurements of the vortex shedding frequencies, these terms cannot be ignored. To study the frequency

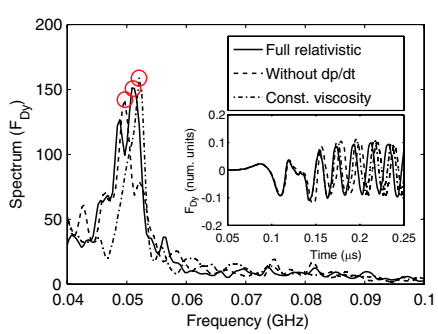

FIG. 4 (color online). Frequencies of the vortex shedding at Re = 3000, using a grid of 2048×1024 cells, are shown. These are calculated for three different cases: the full relativistic, nonrelativistic, and relativistic with constant viscosity. In the inset, the lift force acting on the obstacle as a function of time is shown.

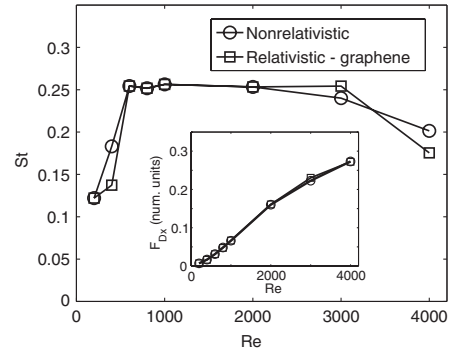

FIG. 5. Strouhal number St as a function of Re for both nonrelativistic and relativistic fluids. In the inset, the mean value of the x component of the drag force as a function of the Reynolds number is shown. The error bar is of the size of the symbol.

of the vortex shedding, we vary the initial velocity in order to obtain different Reynolds numbers. The Strouhal number St is defined as the dimensionless frequency of the vortex shedding and can be calculated as $\mathrm{St} = f_s L/U_{\mathrm{typ}}$, where f_s is the frequency of the vortex shedding. Figure 5 shows that the relation between St and Re is very similar for the relativistic and nonrelativistic fluids, with a fast growth of St in the range $200 < \mathrm{Re} < 1000$, followed by a flattop at St ~ 0.25 [10] for Re > 1000. From the Strouhal number, we can obtain the frequencies of the vortex shedding as $f_s = 0.2U_{\mathrm{typ}}/L$. The frequency of the drag force is twice that of vortex shedding, namely, $f_{Ds} = 0.4U_{\mathrm{typ}}/L$. As a result, once the Reynolds number is known, one can compute the frequency of the drag force, the Strouhal number, and then compare with the FFT of the electric current measurement in the sample. The mean value of the drag force $\bar{F}_{Dx}$, reported in the inset of Fig. 5 as a function of the Reynolds number, shows a monotonic dependence in the range of Re explored here.

Another kind of setup to detect preturbulence in graphene experiments, with the possibility of being implemented nowadays, consists of building a constriction,

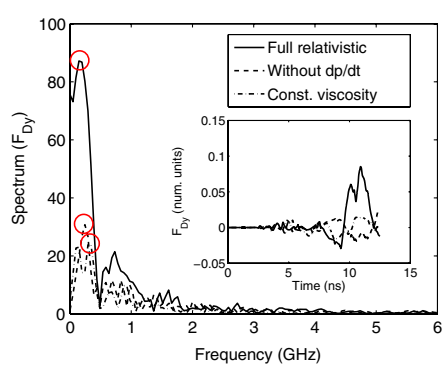

FIG. 6 (color online). The same case of Fig. 4, but in the case of the constriction at Re = 25, using a grid with 1024×1024 cells. Also, the lift force acting on the obstacle as a function of time is shown (inset).

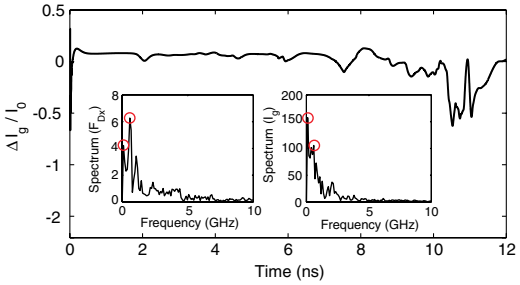

FIG. 7 (color online). The same case as Fig. 3 for the constricted flow at Re = 25. In the inset, the spectrum of the drag force acting on the obstacle (left) and the electric current (right) is shown.

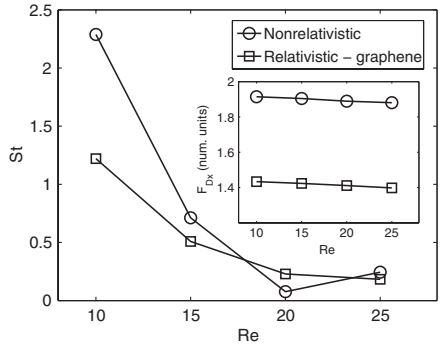

FIG. 8. The same as Fig. 5 for the case of the constriction. In the inset, we show the drag force acting on the obstacle as a function of the Reynolds number.

where the Dirac fluid can develop vorticity patterns as it crosses through. Figure 1 shows the vorticity at Re = 25, where the characteristic length $L = 50$ cells has been chosen as the distance between the tips. In this case, the initial velocity is taken $\vec{u} = (u_x, 0) = (0.0005, 0)$, in lattice units, and the simulation is performed using a grid of 1024×1024 cells. We simulate two systems, one with the full relativistic equations and the other one by just removing the relativistic term $\partial p/\partial t$. From the simulations (see Fig. 1), we conclude that the relativistic contribution affects the time to the onset of instability, and, from Fig. 6, we can appreciate that, as for the circular impurity, the frequency of the vortices presents a shift due to the relativistic corrections. However, both constant viscosity and removal of the relativistic correction contribute to an increase of the frequency of the fluctuations. Figure 7 shows how such fluctuations can be measured and the characteristic frequencies (see red circles in Fig. 7) related with the drag force acting on the constriction. Note that, in order to achieve Re = 25, at a speed of $0.1c$, the distance between tips is about 1.25 μm.

As for the case of the circular impurity, we can find the characteristic relation between the Strouhal number and the Reynolds number for this geometrical setup (see Fig. 8). From the inset of Fig. 8, we observe that the drag force decreases slightly, as the Reynolds number is increased, and exhibits a noticeable difference between the nonrelativistic and relativistic cases.

Summarizing, we have shown that, in the range of Re $\sim 10^2$, vorticity patterns can be indirectly observed by measuring the electric current fluctuations in the graphene sample. However, using a different geometry, like a constriction, signatures of preturbulence can be detected already at Reynolds numbers as small as Re ~ 25. We have also compared the effects of relativistic corrections, such as dynamic compressibility and the dependency of the viscosity on the temperature, on the dynamics of the system. In these cases, the temperature dependency of the viscosity and the term $\partial p/\partial t$ produce a shift in the frequencies of the vortex shedding and, therefore, in the electric current fluctuations. Additionally, the relativistic correction term, $\sim \partial p/\partial t$, is found to delay the instability process in the case of the constricted flow.

We thank K. Ensslin for enlightening discussions. S. S. thanks ETH Zürich for kind hospitality and financial support.

*mmendoza@ethz.ch
†hjherrmann@ethz.ch
‡succi@iac.cnr.it

[1] K. Novoselov, A. Geim, S. Morozov, D. Jiang, M. Katsnelson, I. Grigorieva, and S. Dubonos, Nature (London) **438**, 197 (2005); K. S. Novoselov, A. K. Geim, S. V. Morozov, D. Jiang, Y. Zhang, S. V. Dubonos, I. V. Grigorieva, and A. A. Firsov, Science **306**, 666 (2004).
[2] A. K. Geim and A. H. MacDonald, Phys. Today **60**, No. 8, 35 (2007).
[3] E. Shuryak, Prog. Part. Nucl. Phys. **53**, 273 (2004); P. K. Kovtun, D. T. Son, and A. O. Starinets, Phys. Rev. Lett. **94**, 111601 (2005); G. Policastro, D. T. Son, and A. O. Starinets, *ibid.* **87**, 081601 (2001).
[4] M. Müller, J. Schmalian, and L. Fritz, Phys. Rev. Lett. **103**, 025301 (2009).
[5] M. Mendoza, B. M. Boghosian, H. J. Herrmann, and S. Succi, Phys. Rev. Lett. **105**, 014502 (2010); Phys. Rev. D **82**, 105008 (2010).
[6] S. A. Hartnoll, P. K. Kovtun, M. Müller, and S. Sachdev, Phys. Rev. B **76**, 144502 (2007).
[7] L. Fritz, J. Schmalian, M. Müller, and S. Sachdev, Phys. Rev. B **78**, 085416 (2008).
[8] I. Meric, M. Y. Han, A. F. Young, B. Ozyilmaz, P. Kim, and K. L. Shepard, Nature Nanotech. **3**, 654 (2008).
[9] S. Succi, *The Lattice Boltzmann Equation for Fluid Dynamics and Beyond* (Oxford University Press, New York, 2001); R. Benzi, S. Succi, and M. Vergassola, Phys. Rep. **222**, 145 (1992).
[10] C. H. K. Williamson, J. Fluid Mech. **206**, 579 (1989); Phys. Fluids **31**, 3165 (1988); F. L. Ponta and H. Aref, Phys. Rev. Lett. **93**, 084501 (2004).